Z. Phys. Chem. **225** (2011) 313–324 / **DOI** 10.1524/zpch.2011.0052


# Ni/nano-$TiO_2$ Composite Electrocoatings: Correlation Between Structural Characteristics Microhardness and Wear Resistance

By Stella Spanou and Evangelia A. Pavlatou*

Laboratory of General Chemistry, School of Chemical Engineering, National Technical University of Athens, 9, Heroon Polytechniou Str., Zografos Campus, Athens 15780, Greece

(Received September 8, 2010, accepted in revised form December 7, 2010)

***Electrodeposition / Crystalline Orientation / Microharness / Wear Resistance / Grain Size***

Nanocomposite coatings were obtained by electrochemical codeposition of $TiO_2$ nano-particles (mean diameter 21 nm, Degussa $P_{25}$) with nickel, from an additive-free Watts type bath. Pure Ni and composite Ni-$TiO_2$ coatings were electrolytically deposited under both direct and pulse current conditions and an extended region of electrolysis conditions (pH, current density, $TiO_2$ loading in the bath). Pure Ni deposits were produced under the same experimental conditions for comparison. The aim of this study was to correlate the observed structural characteristics of the coatings (crystallographic orientation and grain size of nickel matrix,) and incorporation percentage with the resulting microhardness values and tribological behavior. Overall, the data have demonstrated that when attributing the observed strengthening effect of composites, not only grain refinement and dispersion strengthening mechanisms, but also preferred crystalline orientation should be taken into consideration. The variation of the wear rate is directly associated with the microhardness variations and consequently, governed by the same parameters that determine the synergistic strengthening mechanism proposed. Pure and composite coatings with [110] crystalline orientation exhibited the highest microhardness values and wear resistance.

## 1. Introduction

$TiO_2$ dispersion-hardened metal electrocoatings show a clear increase of the hardness and wear resistance compared with the pure matrix ones [1–10]. There are a considerable number of research reports concerning the effects of bath composition and operation conditions on the amount of inert particles codeposited with the metal matrix and the resulting properties of the composite coatings [1,2,4,5,8–10]. However, limited research is carried on the effect of codeposited particles on the microstructure [1,2,10] and the correlation between structural characteristics and resulting properties [11].

Concerning $TiO_2$ particle-reinforced Ni composite electrocoatings it has been proven that they exhibit improved mechanical properties [1–4,7–11], accompanied

* Corresponding author. E-mail: pavlatou@chemeng.ntua.gr

by interesting photocatalytic activity as reported by de Tacconi *et al*. [12]. Specifically, the incorporation of $TiO_2$ particles into the nickel matrix leads to the formation of finer structures [13,14], modifies the preferred orientation [10,11,13,14] and lattice defects [10,15], while decreases the residual tensile stresses [16] and increases the hardness [1–4,7–11], the wear [1–4,7–10] and corrosion resistance [1,4,7,9,10,16] of the coatings, compared to pure nickel deposits.

The electrocrystallization of Ni is known to be a highly inhibited process as a consequence of hydrogen codeposition. Depending on plating conditions, mainly pH value of the bath and current density, Amblard *et al*. observed a predominance of a definite inhibitor, which selectively promotes one mode of growth and leads to a deposit exhibiting specific structural characteristics [17]. It has been established that nickel deposits from an additive free Watts type bath under direct current conditions exhibit three inhibited textures [110], [210] and [211] attributed to the presence of atomic, molecular forms of adsorbed hydrogen and colloidal $Ni(OH)_2$ in the catholyte interface, respectively [17]. Moreover, the observed [100] mode of growth is considered to be the most “free” from inhibiting chemical species, presenting few structural defects, maximum ductility and high values of grain size [11,14], low tensile strength, yield strength, and microhardness [11,18–20]. An attempt to formalize a correlation between electrodeposition conditions and the texture of Ni/nano-$TiO_2$ coatings under both direct (DC) and pulse current conditions (PC) has been conducted in our previously published research [11,14].

In this work, extended data of our previously reported study on the microhardness values of pulse deposited composites [11], as well as new experimental data on nanostructured Ni and Ni/nano-$TiO_2$ deposits prepared under direct current conditions are presented, and overall highlight the effect of crystallographic texture on the relationship between crystallites grain size, microhardness and wear resistance.

## 2. Experimental

Pure Ni and composite Ni-$TiO_2$ coatings were electrolytically deposited from an additive-free nickel Watt’s solution under conditions described in Table 1. The electrodeposition experiments were performed on rotating disk electrode (RDE) under direct and pulse current conditions. The $TiO_2$ powder (Degussa P25) with a mean diameter of 21 nm was used as received without any pre-treatment. Titania particles were maintained in suspension by continuous magnetic stirring for at least 24 h before deposition, as well as during the electrolysis process. The concentration of $TiO_2$ particles on the surface was evaluated by using fluorescence X-ray spectroscopy (XRF) [14] and energy dispersive X-ray spectroscopy (EDS) measurements [11]. The preferred orientation of both pure and composite coatings as well as the average Ni grain size was determined as described elsewhere [14]. The thickness of the produced coatings was at least 50 μm in order to obtain preferred orientations fully developed and therefore attain results comparable and reliable.

Measurements of the Vickers microhardness (HV in GPa) of pure nickel and Ni/$TiO_2$ composite deposits were performed on the surface by using a Reichert microhardness tester under 50 g load for 15 s and the corresponding final values were determined as the average of 10 measurements.

**Table 1.** Experimental parameters for the preparation of pure Ni and composite Ni/nano-$TiO_2$ electrocoatings and wear test conditions.

| | |
|---|---|
| **Electrolyte composition** | |
| $NiSO_4 \cdot 6H_2O$ | $300\,g\,L^{-1}$ |
| $NiCl_2 \cdot 6H_2O$ | $35\,g\,L^{-1}$ |
| $H_3BO_3$ | $40\,g\,L^{-1}$ |
| **Electrodeposition conditions** | |
| Temperature (°C) | 50 |
| Substrate | Brass disc (diameter 25 mm) |
| Cathode rotation rate (rpm) | 600 |
| Anode | Ni foil |
| Magnetic stirring (rpm) | 250–320 |
| Direct current (DC) | |
| $TiO_2$ powder Degussa $P_{25}$ ($d_m = 21$ nm) | 20, $100\,g\,L^{-1}$ |
| pH | 1, 2, 3, 3.5, 4, 4.4, 5 |
| Current density ($A\,dm^{-2}$) | 0.5, 1, 2, 5, 10, 20, 40 |
| Pulse current (PC) | |
| $TiO_2$ powder Degussa $P_{25}$ ($d_m = 21$ nm) | $20\,g\,L^{-1}$ |
| pH | 2, 3.5, 4 |
| Current density ($A\,dm^{-2}$) | 1, 5, 20 |
| Duty cycle (d.c) | 50% |
| Frequency (Hz) | 0.1, 1, 10, 100, 1000 |
| **Wear test conditions** | |
| Load | 10N |
| Pin's ball | Corundum ($d = 6$ mm) |
| Ball's linear velocity ($m\,s^{-1}$) | 0.06 |
| Sliding cycles | 5000 |
| Ambient conditions | $T = 25\,°C$ and humidity 50% |

Tribological properties were studied by ball-on-disc measurements using a CSEM tribometer apparatus. All wear tests were performed in ambient conditions against corundum balls, without lubrication. The experimental conditions of tribological measurements are also given in Table 1. The coefficient of friction (cof) was recorded continuously during the sliding tests, while the volumetric wear factor (cw) was calculated as reported in [21].

## 3. Results and discussion

It is well established that Ni/nano-$TiO_2$ composite coatings microhardness and tribological behavior are strongly affected by the volume fraction of the particles codeposited with the metal matrix and, thus a considerable number of efforts have been made to correlate the amount of codeposited particles with the electrodeposition parameters, such as current density [10,11,14] and particles loading in the bath [1–4,9]. This however may be unfortunate since the correlation of property data with nonmetallic particulate inclusion percentages may be erroneous due to synergistic effects arising from other factors such us the modified metal microstructure [22,23]. Therefore, the microhardness and wear resistance of the coatings will be assessed from the viewpoint of crystal orientation, grain size, type of imposed current and nanoparticles codeposition percentage.

### 3.1 Correlation between structural characteristics and microhardness of deposits

Generally, the strengthening mechanisms of polycrystalline metals and composites can be described as follows: (a) grain refinement strengthening from Hall–Petch relationship; (b) dispersion strengthening due to Orowan mechanism; and (c) crystal orientation [24]. Despite the significant number of investigations on the system Ni/nano-$TiO_2$, less attention has been paid to the possible effect of grain orientation on the strengthening mechanism [11]. It should be noticed that in order to obtain a dispersion-strengthening effect, it is crucial to achieve a uniform embedding of non-agglomerated nano-particles in the matrix. It is worth to be mentioned that, according to previous experimental findings by applying HRFE-SEM [25], as well as GDOS [14] techniques the distribution of the $TiO_2$ nano-particles on the surface and within the thickness has been indicated as uniform, without serious problems of agglomeration. In order to elucidate the hardening mechanism of both direct and pulse plated pure and composite nickel coatings, the microhardness values of deposits exhibiting three different textures ([110], [100], Random) have been plotted as a function of the codeposition percentage and the reciprocal square root of average grain size, while the average grain size was varied within the range 15–500 nm.

***Direct current conditions.*** From Fig. 1a it is apparent that an increase of the particles' loading in the bath results in definite increment of nanoparticles in the composite, independently of the applied electrolysis conditions (Fig. 1a). Nevertheless, no explicit relationship between the incorporation percentage and the resulting microhardness values is revealed; a definitely more pronounced effect is apparent in the case of the composites oriented through [100] axis. Unlike to these results, previous studies on Ni/nano-$TiO_2$ electrocoatings have supported a corresponding linear relationship, for however limited number of samples [2–4,8–10]. Given that the [100] textured deposits have been found to be "softer" amongst coatings exhibiting the other three preferred orientations [11,18,19,26], the incorporation of sufficient amount of $TiO_2$ nanoparticles in such a kind of matrix is not expected to efficiently improve the composites' microhardness. At the same time composites exhibiting [110] preferred orientation demonstrate a trend of increasing microhardness values with increasing nanoparticles incorporation rate. This behaviour could be attributed to a dispersion-strengthening mechanism, in which titania nanoparticles inhabit the grain boundaries of the nanocrystalline nickel matrix coatings, and act as obstacles to the grain movement and grain boundaries migration [2,3,27].

According to our previous report concerning deposits prepared under DC conditions, it has been demonstrated that the titania incorporation in the nickel matrix preferably induces the predominance of [100] crystalline orientation [14], and thus the majority of coatings plotted in Fig. 1 is oriented through this axis. The embedding of $TiO_2$ nanoparticles imputes grain refinement, which is more pronounced in the case of

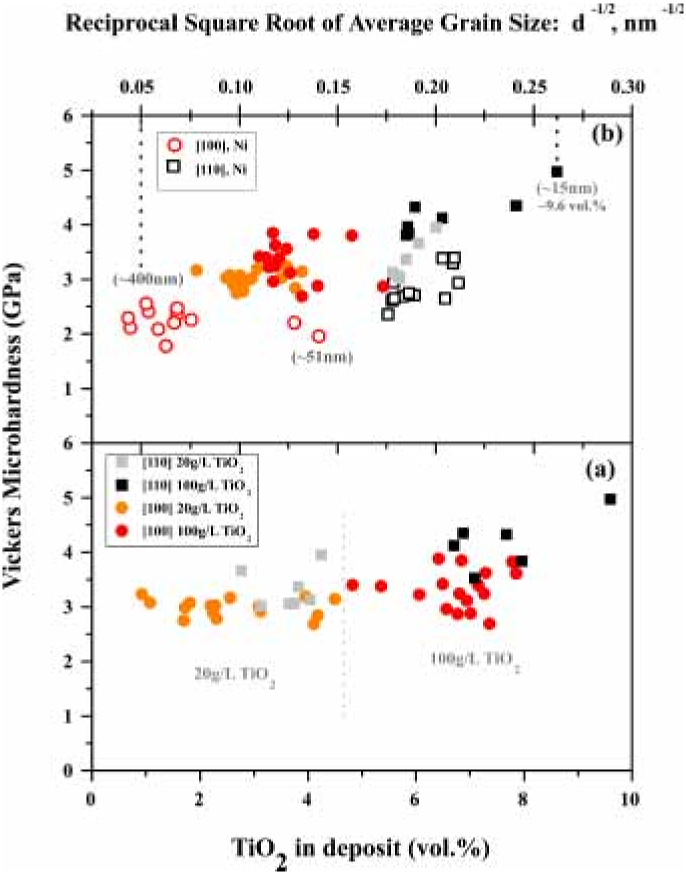


**Fig. 1.** Variation of composites microhardness values with different textures as a function of (**a**) volume percentage of codeposited nano-$TiO_2$ particles in nickel matrix and (**b**) the average grain size ($d^{-1/2}$).

composites with [100] texture (Fig. 1b). Moreover, deposits exhibiting [110] orientation present lower values of average grain size and higher microhardness values compared to the ones oriented through [100] axis, which is consisted with bibliographic data [11,26]. Furthermore, the microhardness of both pure and composite coatings seems to increase with decreasing average grain size. Nevertheless, in the case of pure Ni deposits oriented through [100] axis, no significant variation is detected and thus no obvious grain size dependence is revealed. The highest microhardness value is observed for a composite exhibiting [110] orientation, probably due to the synergistic mechanism involved between dispersion strengthening (highest incorporation value archived i.e. 9.6 vol. %) and grain refinement strengthening (lowest average grain size archived i.e. 15 nm). In order to explain the origin of composites' microhardness variations – for both orientations – that can not be attributed either to grain refinement or dispersion strengthening, nor to their combination, special attention should be paid on the electrolysis conditions (mainly pH) and how they influence the internal stresses, grain-boundary sliding, hydrogen embrittlement and quality of preferred orientation [10,18,28,29]. An attempt to explore the effect of this last parameter will be published elsewhere.

Data from Fig. 1 demonstrated that Ni/nano-$TiO_2$ composite coatings exhibited higher microhardness values compared to pure nickel ones, provided that they exhibit the same preferred orientation and similar average grain size. The experimental data, for the composites prepared under DC conditions, reveal that it is crucial to take into consideration the preferred crystalline orientation in order to define if there is a direct correlation between codeposition rate and microhardness.

***Pulse current conditions.*** Pulse electrodeposition, under specific electrolysis conditions (pH, $J_p$), was performed so as to study the perturbations of Ni crystal growth induced by pulse frequency on Ni/nano$TiO_2$ coatings exhibiting three well developed textures ([110], [100], random), as described extensively in Ref. [11]. It has been proven that composites prepared in the PC regime exhibited higher incorporation percentages than those obtained under DC conditions, and systematically the highest incorporation rates were achieved at pulse frequencies $\nu > 100$ Hz. In Fig. 2 all experimental data concerning the variation of microhardness values as function of volume percentage of codeposited nano-$TiO_2$ particles in nickel matrix (Fig. 2a) and the average grain size ($d^{-1/2}$) (Fig. 2b) are presented.

Specifically, the composite deposits with [100] preferred crystalline orientation exhibit the highest average grain size values among the other deposits and show the lowest values of microhardness, despite the efficient embedment of $TiO_2$ nanoparticles into the matrix (Fig. 2a,b). These results are consisted with those coatings oriented through [100] axis and were prepared under DC conditions (Fig. 1). On the other hand, randomly oriented composites present considerable increase of microhardness in a narrow distribution of mean grain size (Fig. 2b) and codeposition range (Fig. 2a). A similar behaviour was reported recently concerning randomly oriented pure nickel deposits [18]. Additionally, our data demonstrate that composites oriented through [110] axis exhibit enhanced microhardness compared to [100] and randomly oriented ones, as well as the lowest mean crystallite sizes, characterised by a broad range of titania incorporation percentage.

Overall, experimental data revealed that the nickel average grain size for both pure and composite coatings, independently of the type of current imposed, is directly associated to the induced nickel crystalline orientation, where deposits oriented through [110] axis exhibited the lowest mean grain size compared to the other observed preferred orientations. In addition, the dependence of hardness values on the mean grain size (Figs. 1, 2) indicates that for attributing the strengthening effect of composites both grain refinement and dispersion strengthening mechanisms should be taken into account for a given preferred orientation.

## 3.2 Correlation between structural characteristics and wear resistance of deposits

Figure 3 represents the typical evolution of friction coefficient for pure and composite coatings oriented through [110] (Fig. 3a) and [100] axis (Fig. 3a), during sliding against corundum ball under non-lubricated conditions. Irrespective of the presence or

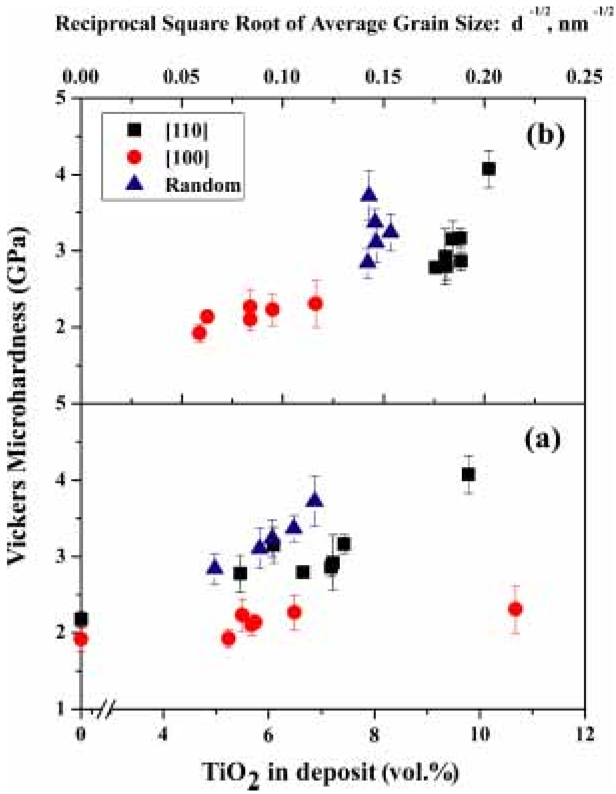


**Fig. 2.** Variation of composites microhardness values with different textures as a function of (**a**) volume percentage of codeposited nano-$TiO_2$ particles in nickel matrix and (**b**) the average grain size ($d^{-1/2}$) [11]. The coatings were produced under an extended region of pulse electrolysis conditions: (■) pH = 4 and $J_p = 1$ A dm$^{-2}$, (•) pH = 3.5 and $J_p = 5$ A dm$^{-2}$, (▲) pH = 2 and $J_p = 20$ A dm$^{-2}$.

not of $TiO_2$ nano-particles in the metal matrix, deposits oriented through [110] axis seem to exhibit higher resistance to sliding at the first 1000 cycles, compared to deposits with the [100] texture. Moreover, it is illustrated that composite coatings demonstrate lower mean friction coefficient values compared to the pure Ni ones, regardless the preferred orientation, which is in agreement with relevant literature [3,7,30,31]. These results indicate that the microstructure design attained by the electrolytic embedding of fine particles into the metal matrix is a simple and effective way to obtain metallic lubricating coatings.

Figure 4 shows the dependence of Vickers microhardness values and wear rate on the preferred orientation and $TiO_2$ nanoparticles content in coatings produced under PC conditions. The data concerning the variation of microhardness values of Ni/nano-$TiO_2$ composites as a function of pulse frequency were published in our recent work [11], however the description of wear rate behaviour as a result of the applied experimental conditions consist new data that contribute to the overall understanding of the systems' intrinsic and non intrinsic properties behaviour.

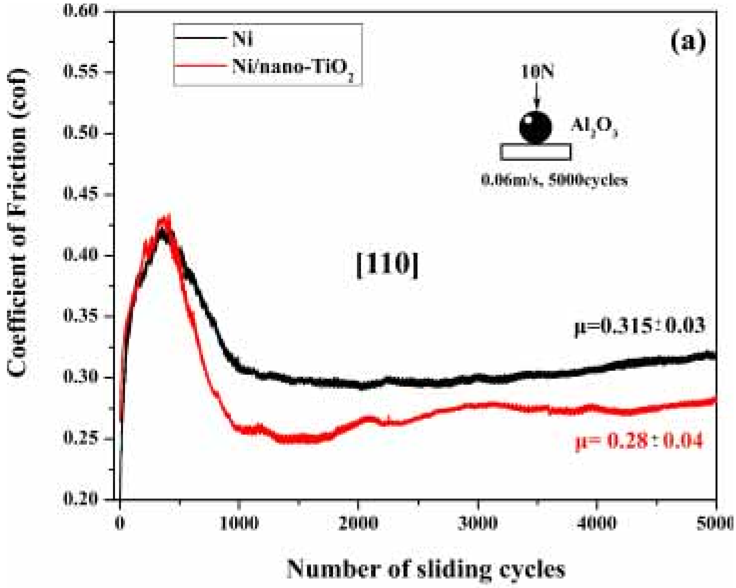


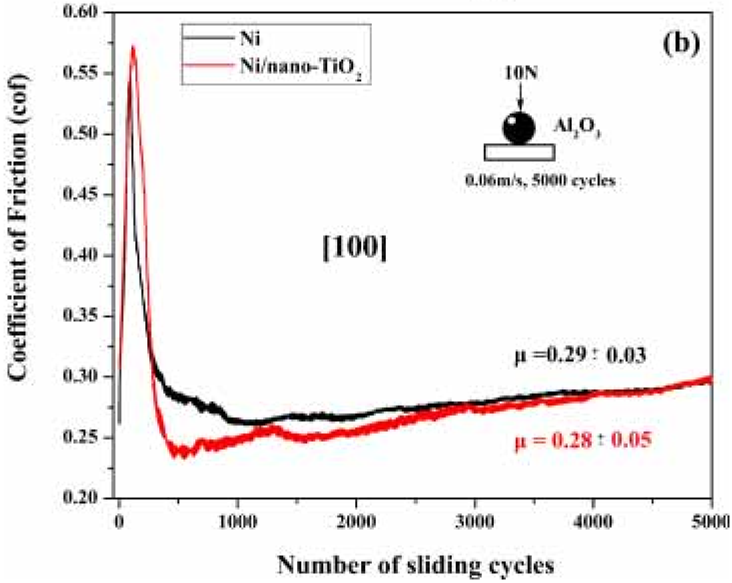


**Fig. 3.** Evolution of friction coefficient for pure Ni and composite Ni/nano-$TiO_2$ coatings sliding against corundum ball ($d = 6$ mm), exhibiting (**a**) the [110] and (**b**) [100] preferred orientation.

All composites prepared under the highest pH and the lowest applied current density value (pH $= 4$, $J_p = 1\ A/dm^2$) as a function of pulse frequency (0.1–1000 Hz) at constant duty cycle (dc $= 50\%$) exhibited the same preferred orientation and increasing values of incorporation percentage, as illustrated in Fig. 4a. The highest microhardness value was obtained at the highest applied frequency, where the highest incor-

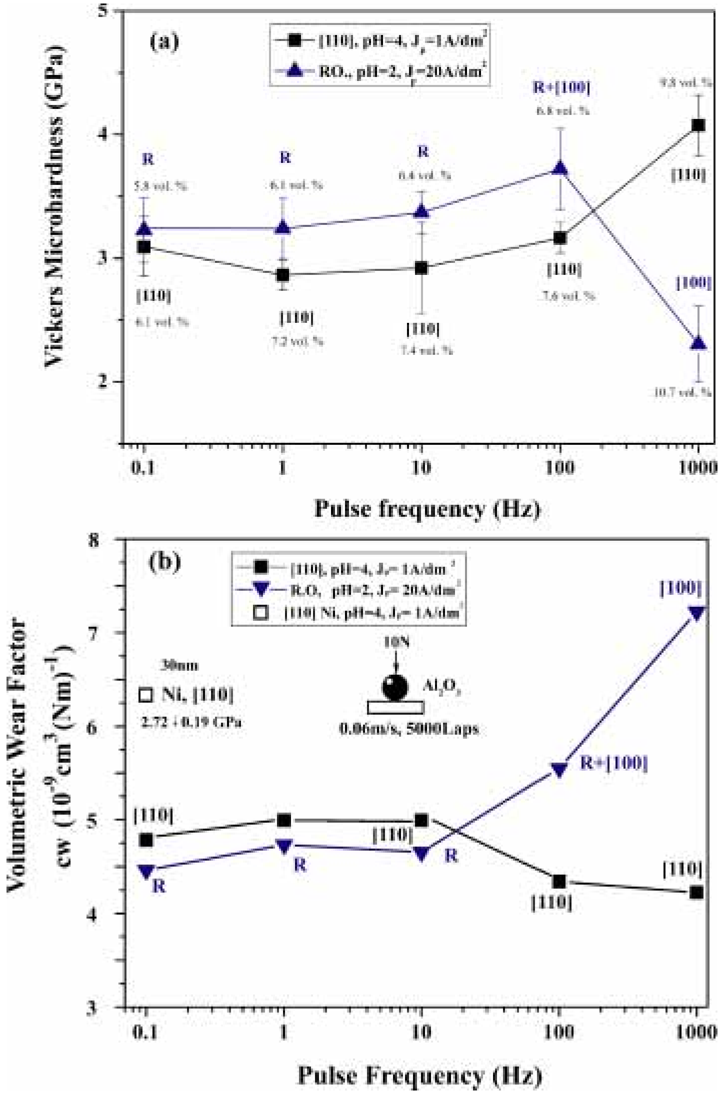

**Fig. 4.** (**a**) Variation of microhardness values [11] and (**b**) volumetric wear factor values of composite Ni/nano-$TiO_2$ coatings prepared under pulse plating conditions as a function of pulse frequency, at a duty cycle of 50%. Composite coatings prepared under the following conditions pH = 4, 2 and $J_p = 1$, 20 A $dm^{-2}$. (Numbers in brackets notify the corresponding nickel preferred orientation of the coating).

poration percentage ($\sim$ 9.8 vol. %) was observed (Fig. 4a). Given that all composites prepared under these experimental exhibit the same preferred orientation accompanied with small variation of mean grain size (22–31 nm, see also Fig. 2b), it is revealed that the leading factor for determining microhardness value is the codeposition rate of nanoparticles in the Ni matrix. On the contrary, the hardness variation as a function of increasing pulse frequency values, under the lowest pH and the highest applied current density (pH $= 2$, $J_p = 20$ A/dm$^2$), has been proven to be directly associated with the imposed preferred orientation and the corresponding average grain size values (Fig. 2). Thus, for applied frequencies $> 10$ Hz the improvement of the quality of "soft" [100] mode of crystalline growth against random one, and the simultaneous increasing of grain size from 42–49 nm to $\sim 74$ nm, result to a considerable decrease of microhardness, despite the fact that under these conditions the highest codeposition rate was achieved $\sim 10.7$ vol. % (Fig. 4a). Thereby, it has been shown that in order to ascribe the observed strengthening mechanism of Ni/nano-$TiO_2$ composites, it is crucial to take into consideration the preferred crystalline orientation of the coatings in combination with grain refinement and dispersion strengthening effect of the nanoparticles.

Additionally, it is revealed that the variation of the wear rate under the aforementioned electrodeposition conditions is directly associated with the microhardness variations and consequently, governed by the same parameters that determine the proposed strengthening mechanism. All coatings exhibiting the highest microhardness values are characterized by low wear rates. However, the imposition of the "soft" [100] texture accompanied by increasing values of grain size results to a substantial increase of the wear rate, which is stimulated by application of increasing values of pulse frequency. The highest wear resistance is observed at the highest applied frequency, where high codeposition rate was observed $\sim 9.8$ vol. % in a nanocrystalline nickel matrix $\sim 21$ nm (Fig. 4b). Moreover, deposits exhibiting [110] mode of growth demonstrated increased wear resistance compared to those exhibiting [100] as expected, if the geometrical characteristics of crystals oriented through axis [100] and [110] are taken into account as proposed by Lampke *et al*. [32]. Finally, pulse plated Ni/nano-$TiO_2$ composite coatings exhibit much lower wear rates than pure nanocrystalline nickel, indicating that the wear resistance of nickel coatings is obviously improved by incorporating titania nanoparticles.

Overall, the experimental data revealed that the application of pulse frequency affected the microhardness and wear resistance of composites by provoking microstructural changes in the deposits, expressed through alterations of crystal growth and corresponding grain size, as well as by varying the amount of codeposited titania nanoparticles with the nickel matrix.

## 4. Conclusions

Concluding, experimental data revealed that the nickel average grain size for both pure and composite coatings, independently of the type of current imposed, is directly associated to the induced nickel crystalline orientation.

Deposits oriented through [110] axis exhibited the lowest mean grain size values compared to the other observed preferred orientations along with higher microhardness and wear resistance. While, the imposition of [100] texture is accompanied by increasing values of grain size, and systematically results to low microhardness values and considerable increase of the wear rate, even after high nanoparticles embedment. The data of this work indicate that the alteration of electrolysis conditions (e.g. particles loading, pH, current density, type of current) in order to increase the titania nanoparticles incorporation percentage in the "soft" [100] Ni matrix does not consequently enhance composites' microhardness.

Ni/nano-$TiO_2$ composite coatings exhibited higher microhardness values compared to pure nickel ones, provided that they exhibit the same preferred orientation and similar average grain size. The observed dependence of hardness values on the mean grain size indicated that for ascribing the strengthening effect of composites both grain refinement and dispersion strengthening mechanisms should be taken into account for a given preferred orientation.

Finally, the application of pulse frequency affected the microhardness and wear resistance of composites by stimulating microstructural changes in the deposits, expressed through alterations of crystal growth and corresponding grain size, as well as by varying the amount of codeposited titania nanoparticles with the nickel matrix.

## References

1. B. Wielage, T. Lampke, M. Zacher, and D. Dietrich, Key Eng. Mater. **384** (2008) 283.
2. D. Thiemig and A. Bund, Surf. Coat. Technol. **202** (2008) 2976.
3. X. J. Sun and Z. J. G. Li, Tribol. Lett. **28** (2007) 223.
4. A. Abdel Aal, Mater. Sci. Eng. A **474** (2008) 181.
5. S. Ramalingam, V. S. Muralidharan, A. Subramania, J. Solid State Electrochem. **13** (2009) 1777.
6. B. Ranjith, G. Paruthimal Kalaignan, Appl. Surf. Sci. **257** (2010) 42–47.
7. Q. Li, X. Yang, L. Zhang, J. Wang, and B. Chen, J. Alloys Compd. **482** (2009) 339.
8. S. A. Lajevardi and T. Shahrabi, Appl. Surf. Sci. **256** (2010) 6775.
9. P. Baghery, M. Farzam, A. B. Mousavi, and M. Hosseini, Surf. Coat. Technol. **204** (2010) 3804.
10. W. Chen, Y. He, and W. Gao, J. Electrochem. Soc. **157** (2010) E122.
11. S. Spanou and E. A. Pavlatou, J. Appl. Electrochem. **40** (2010) 1325.
12. N. R. de Tacconi, C. A. Boyles, and K. Rajeshwar, Langmuir **16** (2000) 5665.
13. T. Lampke, B. Wielage, D. Dietrich, and A. Leopold, Appl. Surf. Sci. **253** (2006) 2399.
14. S. Spanou, E. A. Pavlatou, and N. Spyrellis, Electrochim. Acta **54** (2009) 2547.
15. C. S. Lin, C. Y. Lee, C. F. Chang, and C. H. Chang, Surf. Coat. Technol. **200** (2006) 3690.
16. F. Erler, C. Jakob, H. Romanus, L. Spiess, B. Wielage, T. Lampke, and S. Steinhauser, Electrochim. Acta **48** (2003) 3063.
17. J. Amblard, M. Froment, and N. Spyrellis, Surf. Technol. **5** (1977) 205.
18. A. Godon, J. Creus, S. Cohendoz, E. Conforto, X. Feaugas, P. Girault, and C. Savall, Scripta Mater. **62** (2010) 403.
19. E. A. Pavlatou, M. Raptakis, and N. Spyrellis, Surf. Coat. Technol. **201** (2007) 4571.
20. T. Fritz, M. Griepentrog, W. Mokwa, and U. Schnakenberg, Electrochim. Acta **48** (2003) 3029.
21. P. Gyftou, M. Stroumbouli, E. A. Pavlatou, P. Asimidis, and N. Spyrellis, Electrochim. Acta **50** (2005) 4544.
22. E. A. Pavlatou, M. Stroumbouli, P. Gyftou, and N. Spyrellis, J. Appl. Electrochem. **36** (2006) 385.
23. A. G. McCormack, M. J. Pomeroy, and V. J. Cunnane, J. Electrochem. Soc. **150** (2003) C356.
24. F. Hou, W. Wang, and H. Guo, Appl. Surf. Sci. **252** (2006) 3812.
25. N. Spyrellis, E. A. Pavlatou, S. Spanou, and A. Zoikis-Karathanasis, Trans. Nonferrous Met. Soc. China **19** (2009) 800.
26. A. F. Zimmerman, G. Palumbo, K. T. Aust, and U. Erb, Mater. Sci. Eng. A **328** (2002) 137.
27. A. Jung, Z. H. Natter, Z. R. Hempelmann, and E. Lach, J. Mater. Sci. **44** (2009) 2725.
28. A. M. El-Sherik, U. Erb, G. Palumbo, and K. T. Aust, Scr. Metall. Mater. **27** (1992) 1185.

29. S. C. Tjong and H. Chen, Mater. Sci. Eng. R **45** (2004) 1.
30. X.-S. Liang, J.-H. Ouyang, Y.-F. Li, Y.-M. Wang, Appl. Surf. Sci. **255** (2009) 4316.
31. S. T. Aruna, C. N. Bindu, V. Ezhil Selvi, V. K. William Grips, K. S. Rajam, Surf. Coat. Technol. **200** (2006) 6871.
32. T. Lampke, S. Steinhauser, D. Richter, B. Wielage, Mat.-Wiss. Werkstofftech. **38** (2007) 23.